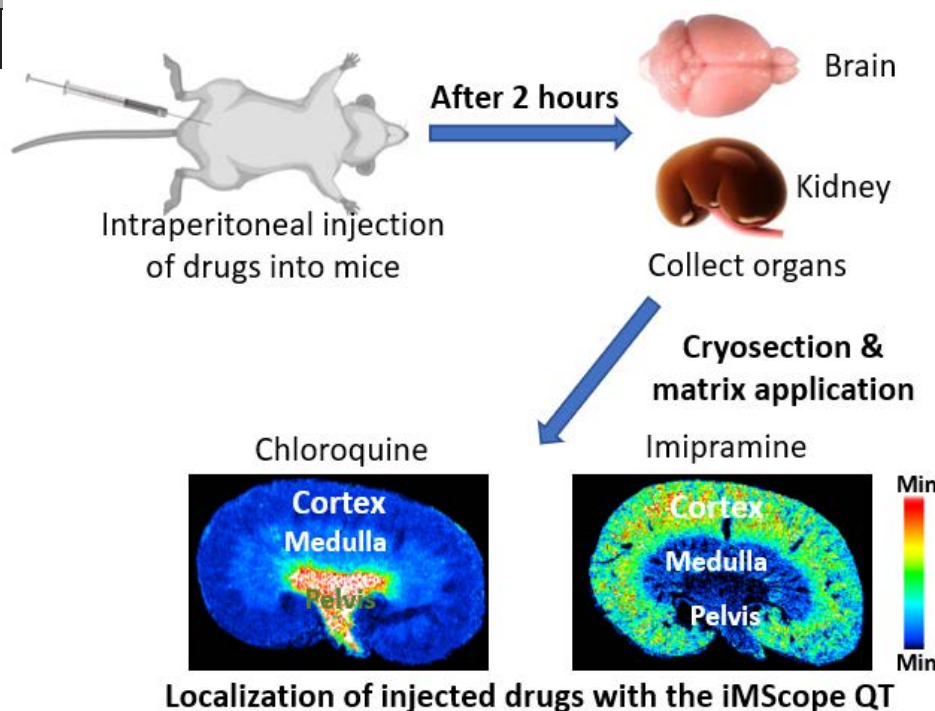


Rapid Mapping of Imipramine, Chloroquine, and Their Metabolites in Mouse Kidneys and Brains Using the iMScope™ QT

Ariful Islam¹, Takumi Sakamoto¹, Qing Zhai¹, Md. Muedur Rahman¹, Md. Al Mamun¹, Yutaka Takahashi^{1,2}, Tomoaki Kahyo^{1,2}, and Mitsutoshi Setou^{1,2}.



■ Abstract

Mass spectrometry imaging (MSI) is a well-known technique for the non-labeling visualization of analytes in biological samples. In this study, we applied a newly developed atmospheric pressure matrix-assisted laser desorption ionization-MSI known as the iMScope QT to rapid (up to 32 pixels/sec) mapping of imipramine, chloroquine, and their metabolites in C57BL/6 male wild-type mice. It revealed region-specific localization of both drugs and their metabolites in the mice's kidneys and brains. Detailed localization information of these drugs and their metabolites observed in our study can aid in understanding clinically-relevant properties, efficacy, and potential side effects of these drugs. Our study also revealed the potential of the iMScope QT for the rapid mapping of small drugs and their metabolites present in the biological samples.

1. Introduction

Mass spectrometry imaging (MSI) techniques continue to gain popularity in various fields, including biological research as well as drug discovery, development, and delivery. The combination of detailed molecular composition and spatial distributions of detected analytes present on sample surfaces makes MSI instruments valuable for extensive characterization of the sample¹. Among the several MSI instruments available, there is an increasing interest in higher-resolution imaging with atmospheric pressure matrix-assisted laser desorption/

ionization MSI (AP-MALDI-MSI) for more focused beams. It simplifies sample preparation when analyzing volatile analytes in addition to other biomolecules at a higher spatial resolution². It can also be used to image analytes with a matrix that would sublime under the high vacuum used in traditional MALDI-MSI³. The Imaging Mass Microscope (iMScope) is an AP-MALDI-MSI instrument developed by Shimadzu, Japan, which is equipped with a built-in optical microscope. It is recognized for its excellent speed and spatial resolution (up to 5 μm)². Recently, Shimadzu have developed another AP-MALDI-MSI instrument known as the iMScope QT, which provides faster imaging with higher sensitivity and spatial resolution.

Imipramine is a well-known drug used to treat depression, anxiety, and nighttime bed-wetting. Chloroquine is also a common drug used to treat malaria, viral diseases, and autoimmune diseases. Although these small drugs are widely used in human health care nowadays, both have several side effects^{4,5}. Localization information of these administered drugs and their metabolites in biological tissues is of paramount importance for better understanding their mode of action and toxic properties. However, there is still a lack of data relating to their localization in different organs. In this study, we tried rapid imaging of these drugs and their metabolites for the first time to explore their distribution in mouse kidneys and brains with the iMScope QT.

¹ Department of Cellular and Molecular Anatomy, Hamamatsu University School of Medicine, Hamamatsu, Shizuoka, Japan.

² International Mass Imaging Center, Hamamatsu University School of Medicine, Hamamatsu, Shizuoka, Japan.

2. Methods

This study aimed to visualize the distribution of imipramine, chloroquine, and their metabolites in C57BL/6JJ male mouse (wild-type, WT) brains and kidneys. Two hours after intraperitoneal injection of imipramine and chloroquine (30 mg/kg of body weight), all mice were dissected following cervical dislocation, and kidney and brain samples were collected rapidly. Thereafter all samples were quickly frozen into dry ice. Then frozen samples were stored at -80 °C. Sagittal sections of mouse kidneys and brains were prepared according to a previously described method⁶⁾ using a CM1950 cryostat (Leica Biosystems, Wetzlar, Germany). For AP-MALDI-MSI, 10 µm thick sections were mounted on Indium Tin Oxide (ITO) coated glass slides (100 Ω, Matsunami, Osaka, Japan).

α-Cyano-4-hydroxycinnamic acid (α-CHCA, Sigma-Aldrich) was used as the matrix, and the matrix was applied using an iMLayer™ matrix vapor deposition system (Fig. 1). The iMLayer chamber was maintained at vacuum conditions during the matrix deposition. Thereafter, MSI data was acquired with the iMScope QT (Imaging Mass Microscope, Shimadzu, Japan) from mouse samples and standard drugs were applied (0.3 µL/spot) on control mouse brain sections.

The iMScope QT combines an atmospheric pressure matrix-assisted laser desorption/ionization (AP-MALDI) source with an LCMS-9030 Q-TOF mass spectrometer (Fig. 2). Prior to measuring the mouse samples, iMScope QT parameters were optimized using standard drugs at two different data acquisition speeds (8 pixels/sec and 20 pixels/sec). The parameters used to acquire data with the iMScope QT are given in Table 1. To confirm detection of the target drugs in the samples, we performed MS/MS imaging of the standard drugs and treated mouse samples with the iMScope QT. For MS/MS imaging of both drugs, 35 V was used for the collision energy, and all other parameters were the same as described for MSI data acquired at 8 pixels/sec (Table 1). Finally, we tried to visualize these drugs and their metabolites with a higher spatial resolution (pitch 25 µm) at a faster speed (32 pixels/sec). MSI data acquisition parameters are given in Table 1.



Fig. 1 iMLayer™ Matrix Vapor Deposition System



Fig. 2 iMScope™ QT Imaging Mass Microscope

3. Results and Discussion

We optimized iMScope QT parameters and acquired AP-MALDI-MSI data in positive ion mode from standard drugs applied to control mouse brain sections (0.3 µL/spot) at two different data acquisition speeds, 8 pixels/sec and 20 pixels/sec. With the iMScope QT, we detected both drugs at a 0.1 µg/mL concentration at both data acquisition speeds (Fig. 3). Interestingly, data acquisition speed did not drastically affect the signal intensity of either drug (Fig. 3, 4).

In a recent study, we reported that these drugs can also be detected by desorption electrospray ionization MSI (DESI-MSI) with higher sensitivity at the usual speed (2 pixels/sec), but sensitivity was drastically affected at higher data acquisition speeds⁷⁾. MALDI-MSI data was also acquired in positive ion mode with a 7T Solarix FT-ICR using three different matrices and different methods, but none of these drugs were detected in our experiments⁷⁾.

Table 1 MSI Analysis Parameters

Setting	8 pixels/sec	20 pixels/sec	32 pixels/sec
Polarity	Positive	Positive	Positive
<i>m/z</i> range	150 - 550	150 - 550	150 - 550
Mass resolution	32000	32000	32000
Spatial resolution (X x Y)	50 µm x 50 µm	50 µm x 50 µm	25 µm x 25 µm
Laser diameter settings	2	2	2
Laser power	65	65	60
Laser shots	100	100	20
Repetition number (Hz)	1000	10000	10000
Detector voltage (kV)	2.4	2.4	2.4
DL temperature (°C)	300	300	300

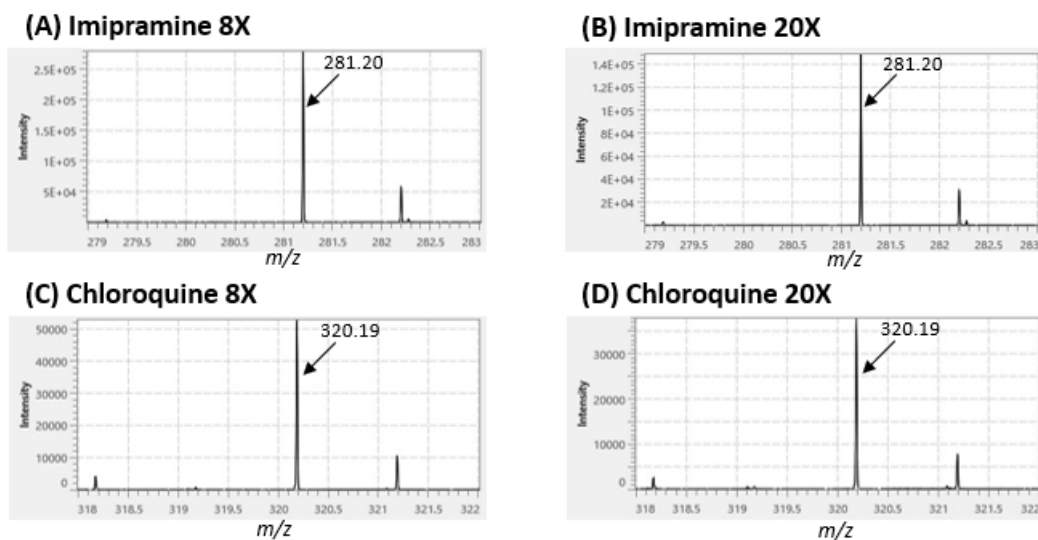


Fig. 3 Effects of data acquisition speed on the sensitivity of iMScope QT for imipramine (A-B) and chloroquine (C-D).

Detection of drugs at different data acquisition speeds by iMScope QT

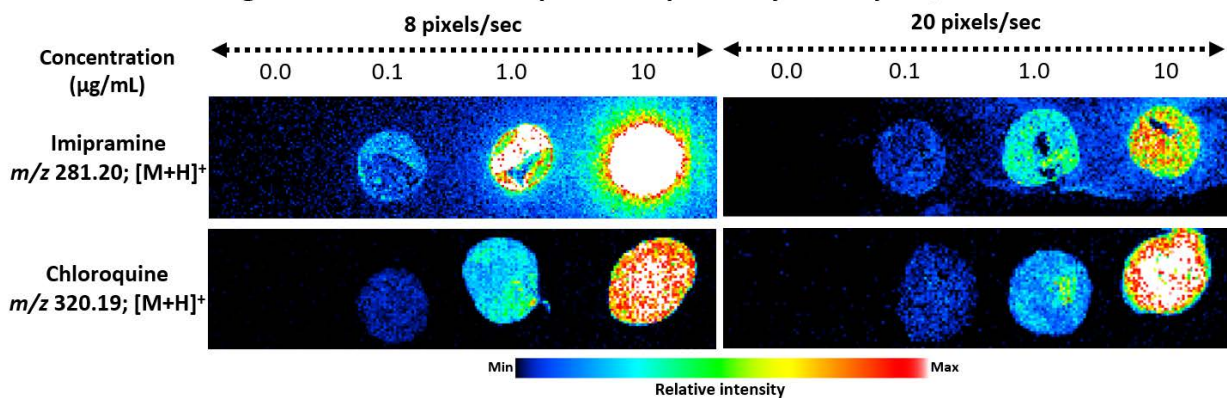


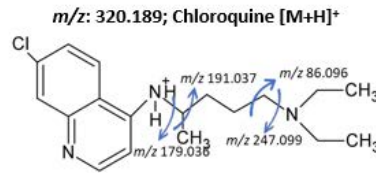
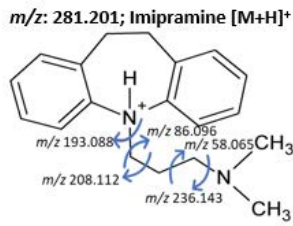
Fig. 4 Ion images of imipramine and chloroquine detected with the iMScope QT at different speeds.

Thereafter we acquired AP-MALDI-MSI data from mouse kidney samples by applying iMScope QT (8 pixels/sec). With the iMScope QT, both drugs were detected as protonated ions not only in the standards but in treated mouse samples. For further confirmation of the detection of these drugs, we used the iMScope QT to perform tandem mass spectrometry (MS/MS) imaging of selected m/z peaks corresponding to imipramine and chloroquine (Fig. 5).

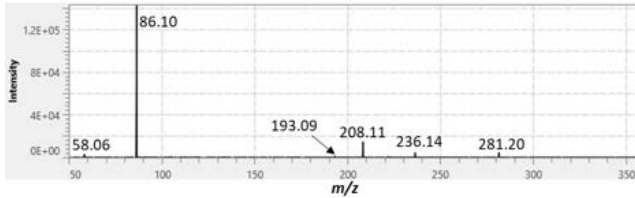
The iMScope QT revealed the distribution of both drugs and their metabolites in treated mouse kidneys for the first time. We noted that imipramine was highly accumulated in the renal cortex, and its metabolites desipramine and 2-hydroxy-imipramine were accumulated in the outer renal medulla and renal pelvis of treated mice (Fig. 6A). We also observed that chloroquine, desethylchloroquine, and chloroquine-M-(C₂H₅)₂ were accumulated mainly in the pelvis and in small amounts in the inner medulla of treated mouse kidneys (Fig. 6B). The renal cortex connects blood vessels to the nephrons. It is associated with the production of red blood cells. The renal medulla consists of renal pyramids, which contain a dense network of nephrons, the functional units of the kidney. The renal pelvis collects urine from the renal pyramid. All these parts of the kidney play essential roles in filtering blood, maintaining electrolyte balance, and removing waste products from the body. As kidneys are commonly exposed to drugs and their metabolites present in blood, drug-induced toxicity in the kidney is common worldwide⁸. Accumulated imipramine and its metabolites in the kidney as observed in our study can show toxic effects by inducing glomerulonephritis and inflammatory cell infiltration⁹.

Additionally, chloroquine and its metabolites as observed in our study might be associated with renal damage by increasing lipid peroxidation and decreasing antioxidant enzyme activities¹⁰. However, further research is required to explore the detailed toxic effects of those accumulated drugs and their metabolites in the specific kidney regions observed. We also explored the localization of imipramine, chloroquine, and their metabolites in mouse brains with the iMScope QT. We observed imipramine and its metabolites throughout the brain, but a somewhat higher amount of imipramine was observed in the thalamus, hypothalamus, septum, and hindbrain of treated mice (Fig. 7A). Imipramine is commonly used to treat anxiety and depression. According to previous reports, accumulated imipramine in these brain regions might inhibit the reuptake of serotonin and norepinephrine and help to relieve anxiety and depression¹¹. Our study also explored a considerable accumulation of chloroquine and its metabolites in the lateral ventricle, 4th ventricle, and fornix of treated mice brains (Fig. 7B). The choroid plexus in the lateral ventricle and 4th ventricle produces cerebrospinal fluid, which plays a vital role in maintaining central nervous system homeostasis¹². It regulates the volume of the brain and cranial cavity, eliminates waste metabolites and unnecessary substances, and transports proteins, nutrients, and drugs^{12,13}. The fornix, a bundle of white matter, plays a critical role in cognitive function by connecting several nodes of limbic circuitry¹⁴. Imipramine and its metabolites increase the production of inflammatory cytokines (IL 1- β and TNF- α) and nitric oxide by microglia⁵. Chloroquine and its metabolites are also known for neurotoxic effects such as psychosis, seizure, disorientation, and hallucination⁴.

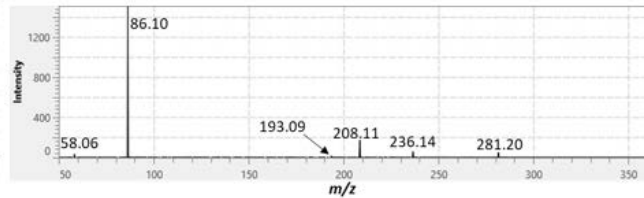
(A) Imipramine, chloroquine, and their possible fragmentation patterns



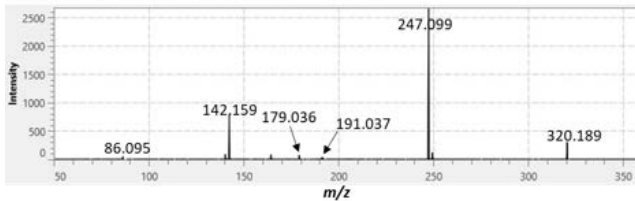
(B) MS² spectra of standard imipramine



(C) MS² spectra of imipramine detected from the mouse kidneys



(D) MS² spectra of standard chloroquine



(E) MS² spectra of chloroquine detected from the mouse kidneys

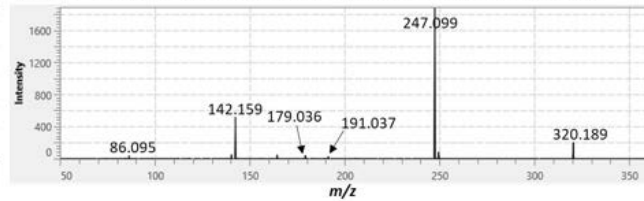
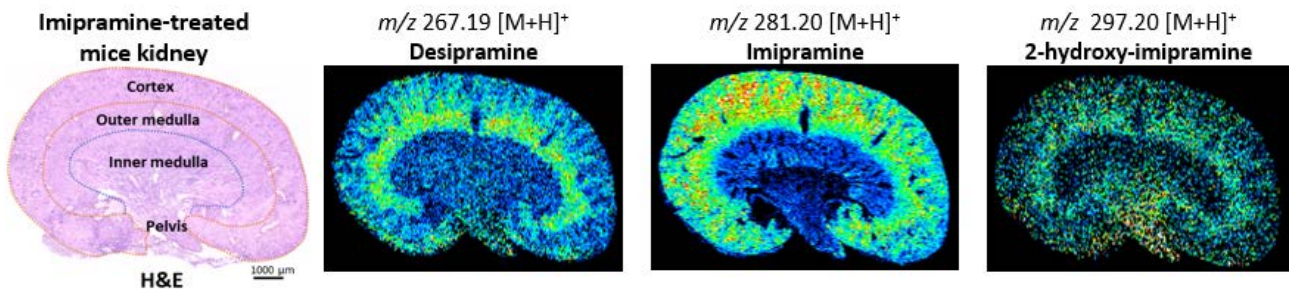


Fig. 5 MS/MS spectra of imipramine and chloroquine detected in standards and treated mouse kidneys using the iMScope QT.

- (A) Possible fragmentation pattern of imipramine and chloroquine.
- (B-C) MS/MS spectra of imipramine detected from standard and treated mouse kidneys.
- (D-E) MS/MS spectra of chloroquine detected from standard and treated mouse kidneys.

(A) Imipramine and its metabolites detected in the mouse kidneys



(B) Chloroquine and its metabolites detected in the mouse kidneys

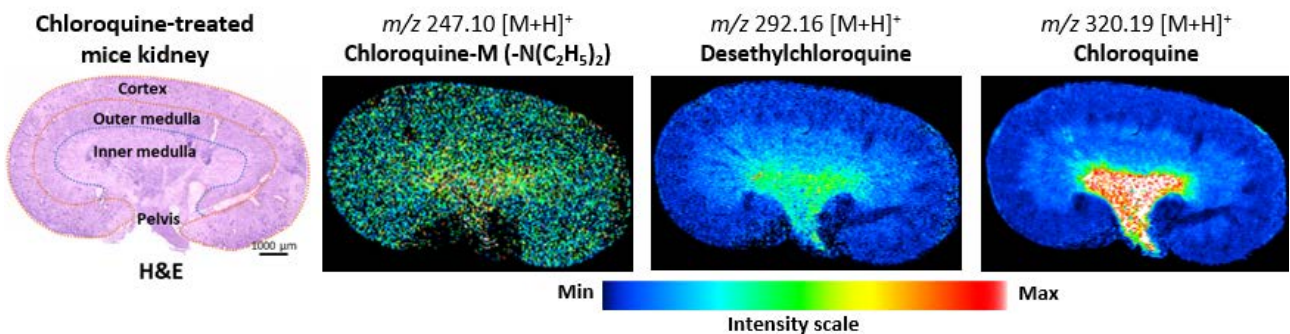
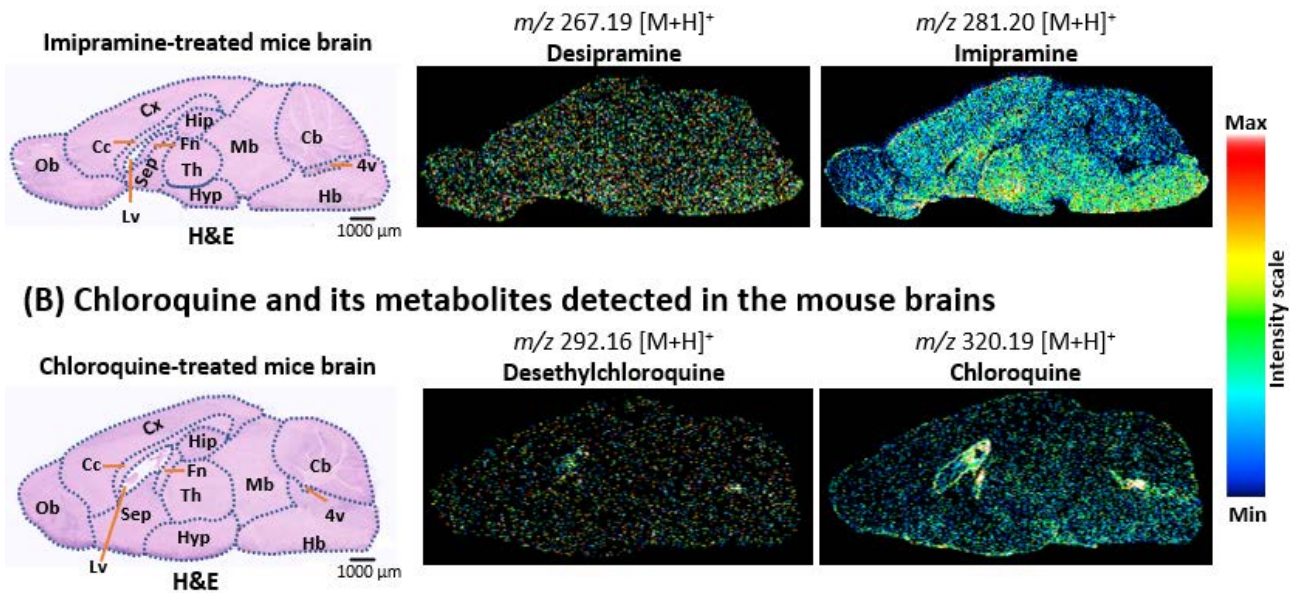


Fig. 6 Localization of imipramine, chloroquine, and their metabolites in the kidneys of treated mice using the iMScope QT.

- (A) Distribution of imipramine and its metabolites in the treated mouse kidneys.
 - (B) Distribution of chloroquine and its metabolites in the treated mouse kidneys.
- Here, the spatial resolution was 50 μm x 50 μm (X, Y), and the data acquisition speed was 8 pixels/sec.

(A) Imipramine and its metabolites detected in the mouse brains



(B) Chloroquine and its metabolites detected in the mouse brains

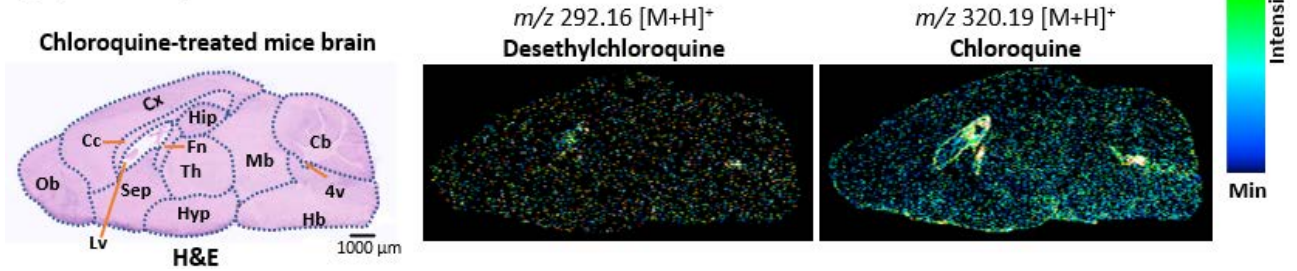


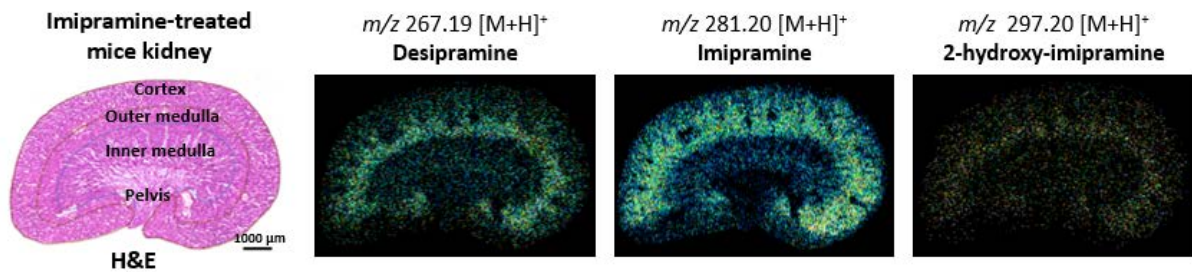
Fig. 7 Localization of imipramine, chloroquine, and their metabolites in the brains of treated mice using the iMScope QT.

(A) Distribution of imipramine and its metabolites in the treated mouse brains.

(B) Distribution of chloroquine and its metabolites in the treated mouse brains.

Here, the spatial resolution was 50 µm 50 µm (X, Y), and the data acquisition speed was 8 pixels/sec. Cb: cerebellum; Hb: hindbrain; Mb: midbrain; Hip: hippocampus; Cx: cerebral cortex; Th: thalamus; Fn: fornix; Cc: corpus callosum; Ob: olfactory bulb; Sep: septum; Hyp: hypothalamus; Lv: lateral ventricle; and 4v: 4th ventricle.

(A) Rapid detection of imipramine and its metabolites in the mouse kidneys by iMScope QT



(B) Rapid detection of chloroquine and its metabolites in the mouse kidneys by iMScope QT

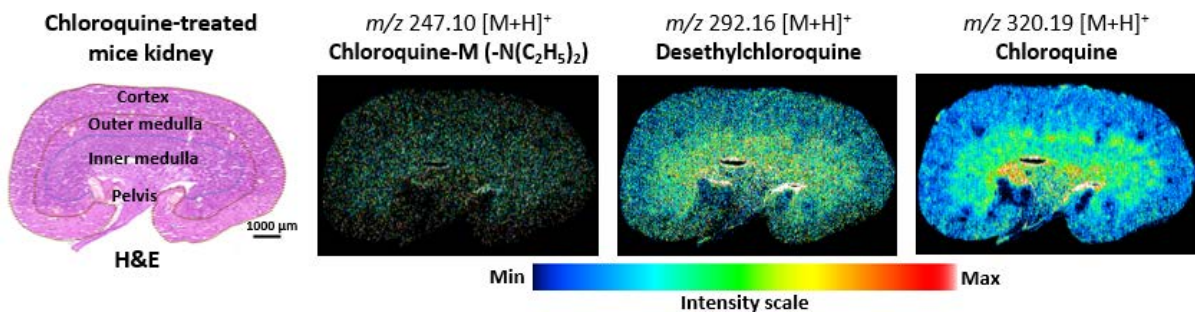


Fig. 8 Rapid localization of imipramine, chloroquine, and their metabolites in the kidneys of treated mice with higher spatial resolution using the iMScope QT.

(A) Distribution of imipramine and its metabolites in the mouse kidneys using higher data acquisition speed.

(B) Distribution of chloroquine and its metabolites in the mouse kidneys using higher data acquisition speed.

Here, the spatial resolution was 25 µm 25 µm (X, Y), and the data acquisition speed was 8 pixels/sec.

As both imipramine and chloroquine can cause neurotoxicity, the accumulation of these drugs and their metabolites in the different brain regions observed in this study might be responsible for the neurotoxic effects and disruption of functions in these regions. Further studies are required to explore the detailed mechanisms of action of these accumulated drugs and drug metabolites associated with brain function and health.

In this study, we also observed that acquiring data at a higher speed (20 pixels/sec) with the newly developed iMScope QT does not significantly affect the sensitivity. Therefore, we tried to visualize imipramine, chloroquine, and their metabolites at much higher data acquisition speed (32 pixels/sec) and higher spatial resolution (25 μm x 25 μm ; X, Y) with the iMScope QT. At this speed and spatial resolution, we detected both drugs and most of their metabolites in treated mouse kidneys with a clear distribution (Fig. 8). We conclude that this MSI instrument can be a good option for users to carry out rapid imaging of drugs, metabolites, and other analytes with high spatial resolution. However, this time we used only two drugs, imipramine, and chloroquine. For other compounds, including medical drugs, MALDI-MSI and DESI-MSI may offer much better sensitivity compared to the iMScope QT. In the future, we will test rapid imaging of other compounds and drugs by applying different MSI tools with a high spatial resolution.

4. Conclusion

For the first time, we revealed the localization of imipramine, chloroquine, and their metabolites in the mice kidneys and brains by applying a newly developed AP-MALDI-MSI instrument known as the iMScope QT, which offers rapid data acquisition with higher sensitivity. Our findings may be helpful in exploring the mode of action and toxic properties of these drugs. Additionally, our study demonstrates the capabilities of the iMScope QT in rapid imaging of analytes present in biological samples.

Acknowledgments

We are sincerely grateful to Satoshi Kasamatsu and Koretsugu Ogata from Shimadzu, Japan for technical support and guidance on the iMScope QT.

<References>

- 1) Buchberger, A.R.; DeLaney, K.; Johnson, J.; Li, L. Mass spectrometry imaging: a review of emerging advancements and future insights. *Analytical chemistry* 2018, 90, 240.
- 2) Harada, T.; Yuba-Kubo, A.; Sugiura, Y.; Zaima, N.; Hayasaka, T.; Goto-Inoue, N.; Wakui, M.; Suematsu, M.; Takeshita, K.; Ogawa, K. Visualization of volatile substances in different organelles with an atmospheric-pressure mass microscope. *Analytical chemistry* 2009, 81, 9153-9157.

- 3) Jackson, S.N.; Muller, L.; Roux, A.; Oktem, B.; Moskovets, E.; Doroshenko, V.M.; Woods, A.S. AP-MALDI mass spectrometry imaging of gangliosides using 2, 6-dihydroxyacetophenone. *Journal of The American Society for Mass Spectrometry* 2018, 29, 1463-1472.
- 4) Doyno, C.; Sobieraj, D.M.; Baker, W.L. Toxicity of chloroquine and hydroxychloroquine following therapeutic use or overdose. *Clinical Toxicology* 2021, 59, 12-23.
- 5) Obuchowicz, E.; Bielecka-Wajdman, A.; Zieliński, M.; Machnik, G.; Gólyszny, M.; Ludyga, T. Imipramine and venlafaxine differentially affect primary glial cultures of prenatally stressed rats. *Frontiers in Pharmacology* 2020, 10, 1687.
- 6) Islam, A.; Takeyama, E.; Mamun, M.A.; Sato, T.; Horikawa, M.; Takahashi, Y.; Kikushima, K.; Setou, M. Green nut oil or DHA supplementation restored decreased distribution levels of DHA containing phosphatidylcholines in the brain of a mouse model of dementia. *Metabolites* 2020, 10, 153.
- 7) Islam, A.; Sakamoto, T.; Zhai, Q.; Rahman, M.M.; Mamun, M.A.; Takahashi, Y.; Kahyo, T.; Setou, M. Application of AP-MALDI Imaging Mass Microscope for the Rapid Mapping of Imipramine, Chloroquine, and Their Metabolites in the Kidney and Brain of Wild-Type Mice. *Pharmaceuticals* 2022, 15, 1314.
- 8) Pazhayattil, G.S.; Shirali, A.C. Drug-induced impairment of renal function. *International journal of nephrology and renovascular disease* 2014, 7, 457.
- 9) Chang, G.-R.; Hou, P.-H.; Wang, C.-M.; Lin, J.-W.; Lin, W.-L.; Lin, T.-C.; Liao, H.-J.; Chan, C.-H.; Wang, Y.-C. Imipramine Accelerates Nonalcoholic Fatty Liver Disease, Renal Impairment, Diabetic Retinopathy, Insulin Resistance, and Urinary Chromium Loss in Obese Mice. *Veterinary sciences* 2021, 8, 189.
- 10) Murugavel, P.; Pari, L. Attenuation of Chloroquine-Induced Renal Damage by α -Lipoic Acid: Possible Antioxidant Mechanism. *Renal failure* 2004, 26, 517-524.
- 11) Yang, J.; Hellerstein, D.J.; Chen, Y.; McGrath, P.J.; Stewart, J.W.; Peterson, B.S.; Wang, Z. Serotonin-norepinephrine reuptake inhibitor antidepressant effects on regional connectivity of the thalamus in persistent depressive disorder: evidence from two randomized, double-blind, placebo-controlled clinical trials. *Brain communications* 2022, 4, fcac100.
- 12) Wichmann, T.O.; Damkier, H.H.; Pedersen, M. A Brief Overview of the Cerebrospinal Fluid System and Its Implications for Brain and Spinal Cord Diseases. *Frontiers in Human Neuroscience* 2021, 15.
- 13) Matsumae, M.; Sato, O.; Hirayama, A.; Hayashi, N.; Takizawa, K.; Atsumi, H.; Sorimachi, T. Research into the physiology of cerebrospinal fluid reaches a new horizon: intimate exchange between cerebrospinal fluid and interstitial fluid may contribute to maintenance of homeostasis in the central nervous system. *Neurologia medico-chirurgica* 2016, 56, 416-441.
- 14) Senova, S.; Fomenko, A.; Gondard, E.; Lozano, A.M. Anatomy and function of the fornix in the context of its potential as a therapeutic target. *Journal of Neurology, Neurosurgery & Psychiatry* 2020, 91, 547-559.

iMLayer and iMScope are trademarks of Shimadzu Corporation or its affiliated companies in Japan and other countries.



Shimadzu Corporation

www.shimadzu.com/an/

For Research Use Only. Not for use in diagnostic procedures.

This has not been approved or certified as a medical device under the Pharmaceutical and Medical Device Act of Japan.

It cannot be used for the purpose of medical examination and treatment or related procedures.

This publication may contain references to products that are not available in your country. Please contact us to check the availability of these products in your country.

The content of this publication shall not be reproduced, altered or sold for any commercial purpose without the written approval of Shimadzu. See <http://www.shimadzu.com/about/trademarks/index.html> for details.

Shimadzu disclaims any proprietary interest in trademarks and trade names other than its own.

Third party trademarks and trade names may be used in this publication to refer to either the entities or their products/services, whether or not they are used with trademark symbol "TM" or "®".

The information contained herein is provided to you "as is" without warranty of any kind including without limitation warranties as to its accuracy or completeness. Shimadzu does not assume any responsibility or liability for any damage, whether direct or indirect, relating to the use of this publication. This publication is based upon the information available to Shimadzu on or before the date of publication, and subject to change without notice.

First Edition: Mar 2023